Biophysical Chemistry 19 (1984) 147–161
Elsevier

BPC 00836

Mg^{2+}-INDUCED PROTON RELEASE FROM *ESCHERICHIA COLI* RIBOSOME AND RIBOSOMAL RNA

Hiroyuki HAGIHARA, Kazuo HORIE, Akira WADA and Hideo FUKUTOME

Department of Physics, Faculty of Science, Kyoto University, Kyoto 606, Japan

Received 1st June 1983
Revised manuscript received 1st November 1983
Accepted 8th November 1983

Key words: Ribosome; Ribosomal RNA; Mg^{2+}; Proton titration; Ion binding; Electrostatic effect

Escherichia coli ribosome released protons upon addition of Mg^{2+}. The Mg^{2+}-induced proton release was studied by means of the pH-stat technique. The number of protons released from a 70 S ribosome in the Mg^{2+} concentration range 1–20 mM was about 30 at pH 7 and 7.6, and increased to about 40 at pH 6.5. The rRNA mixture extracted from 70 S ribosome showed proton release of amount and of pH dependence similar to those of the 70 S ribosome but the ribosomal protein mixture released few. This indicates that rRNA is the main source of the protons released from ribosome. The pH titration of rRNA showed that the pK_a values of nucleotide bases were downward shifted upon Mg^{2+} binding. This pK_a shift can account for the proton release. The Scatchard plots of proton release from rRNA and ribosome were concave upward, showing that the Mg^{2+}-binding sites leading to proton release were either heterogeneous or had a negative cooperativity. A model assuming heterogeneous Mg^{2+}-binding sites is shown to be unable to explain the proton release. Electrostatic field effect models are proposed in which Mg^{2+} modulates the electrostatic field of phosphate groups and the potential change induces a shift of the pK_a values of bases that leads to the proton release. These models can explain the main features of the proton release.

1. Introduction

The ribsome is a complicated polyelectrolytic system consisting of RNAs and proteins. The polyelectrolytic interaction of ribosome with metal ions plays important roles in its structure and functions [1–4]. Some studies have been made on the binding of metal ions, especially Mg^{2+}, to ribosome [5–7]. However, little is understood about the state of ionizable groups in the ribosome and how they are affected by metal ions. Only a few studies have been made on ionizable groups in rRNA and ribosome. A pH titration study of rRNA revealed the existence of a metastable structure in an acid pH region [8]. The charge of the ribosome was studied as a function of bound Mg^{2+} and H^+ [3]. Kliber et al. [9] found that the pH titration of ribosome was affected by the binding of Mg^{2+} and K^+. They also found that ribosome released protons upon binding of Mg^{2+} and K^+.

The Mg^{2+}- or K^+-induced proton release from ribosome found by Kliber et al. is a phenomenon directly reflecting the effect of metal ions on ionizable groups. In this paper, we present a study on the Mg^{2+}-induced proton release from *Escherichia coli* ribosome with the aims to identify the main source of the protons and to clarify the mechanism of the proton release. For this purpose we measured pH titration and Mg^{2+}-induced proton release, including its pH dependence, of 70 S ribosome, rRNA and ribosomal protein. The pH-stat method was used for detection of released protons. The data showed that rRNA was the main source of the Mg^{2+}-induced proton release. We propose polyelectrolytic models for the proton release. In these models, the proton release is explained as being due to change of the Coulombic field of the

phosphate backbone by polyelectrolytic binding of metal ions. The change of the Coulombic field brings about a shift of pK_a values of ionizable nucleotide bases and consequently proton release from bases. The models are shown to be able to explain the data for rRNA.

2. Materials and methods

2.1. Bacterial cells and ribosomes

E. coli strain Q 13 was grown at 37°C and harvest in the mid-log phase. High-salt-washed ribosomes were prepared according to a procedure described earlier [10], rapidly frozen in liquid N_2 and stored at −20°C in the standard buffer with 100 mM NH_4OAc, 10 mM $Mg(OAc)_2$, 20 mM Tris-HCl (pH 7.6) and 6 mM 2-mercaptoethanol.

2.2. rRNA and ribosomal proteins

rRNAs were extracted from the high-salt-washed ribosomes by the phenol-sodium dodecyl sulfate method [11], so that the sample was an equimolar mixture of 23 S, 16 S an 5 S rRNAs. It was rapidly frozen and stored at −20°C in 360 mM KCl, 20 mM $MgCl_2$ and 20 mM Tris-HCl (pH 7.6). A mixture of ribosomal proteins was prepared from the high-salt-washed ribosomes by the acetic acid method [12] and stored at −20°C in 8 M urea.

2.3. Determination of concentrations

The concentration of ribosome (rRNA) was determined from the absorbance in 100 mM KCl, 10 mM (1 mM for rRNA) $MgCl_2$ and 20 mM Tris-HCl (pH 7.6), assuming that 1 A_{260} unit * equals 26 pmol 70 S ribosomal particle (rRNA) [13]. The concentration of the ribosomal protein mixture was determined by the microbiuret method [14] using bovine serum albumin as a standard. The concentration of stock $MgCl_2$ solution (2 M) was measured by the Eriochrome black T method [15].

2.4. Potentiometric measurements

pH titrations and pH-stat measurements were carried out with a Radiometer TTT2b titrator and an ABU12 autoburet. A glass electrode (G2222C) and a calomel electrode (K4112) were used for the 5 ml cell; G202C and K401 electrodes were used for the 25 ml cell. The buret volume was 0.25 ml and the precision of titrant volume was about 1 μl. To avoid the effect of dissolved CO_2, the cell with sample solution was continuously flushed from 15 min before a measurement with N_2 gas previously washed with water. The cell was immersed in a thermostated (25.0°C) water bath, which was shielded electrically, and stirred by a magnetic stirrer. The titrant used in the pH titration and pH-stat was 0.1–0.005 N KOH. Before and after each experiment the concentration of titrant was calibrated by a 0.01 N HCl standard solution. In a pH titration, the pH was recorded with a Watanabe WX4402 XY recorder as a function of time during a constant supply of KOH through the autoburet.

The Mg^{2+}-induced proton release was measured by the pH-stat method. The sample solution (20 ml) containing 500–530 A_{260} units of high-salt-washed ribosomes was adjusted to a given pH by adding 0.1 N HCl or 0.1 N KOH. Then $MgCl_2$ solution (2 M) was added stepwise, 5–20 μl per injection, through a microsyringe and the pH was readjusted automatically to the initial value by adding 0.01 N KOH through the autoburet. A blank experiment using a solution without ribosomes was also carried out. The net amount of added KOH subtracted from the blank is equal to the amount of protons released from ribosomes upon addition of Mg^{2+}. The error of the pH-stat method was less than 5 protons per 70 S particle in the pH region from 6.5 to 7.6.

In the cases of the rRNA and ribosomal protein mixtures, the amount of sample used in each experiment was about 360 A_{260} units and about 4 mg, respectively. In pH titration measurements, the amount of sample in each experiment was half of (for ribosome and rRNA), or equal to (for ribosomal protein), that in pH-stat measurements.

2.5. Preparation of unbuffered samples

A stock solution of 70 S ribosomes was dialysed against 100 mM KCl and 10 mM $MgCl_2$ in a

* A_{260} unit, the quantity of material contained in 1 ml of a solution measured with the absorbance at 260 nm.

closed vessel at 4°C for 5–7 h with one exchange of dialysate in the course of the dialysis. The dialysate was maintained at about pH 7–8 with 0.1 N KOH. The dialysed material was used as an unbuffered sample for a titration or a proton release experiment. The initial concentration of Mg^{2+} in a proton release experiment was set to 1 or 2 mM by dilution immediately before measurement of proton release in order to avoid inactivation and degradation of ribosomes due to low Mg^{2+} concentration [16]. A stock solution of the rRNA mixture was dialysed against 100 mM KCl (and 10 mM $MgCl_2$ in some cases) for about 4 h as described above. A stock solution of the ribosomal protein mixture was dialysed against 6, 1 or 0.2 M guanidine hydrochloride for at least 15 h as described above. 100 mM KCl was present in the cases of 1 and 0.2 M guanidine hydrochloride. Then, the pH of the dialysate was maintained at about 7 to avoid precipitation of proteins.

2.6. Activities of ribosome

The activity of 70 S particle formation was measured by 5–20% sucrose density gradient centrifugation in buffer consisting of 100 mM NH_4OAc, 15 mM $Mg(OAc)_2$ and 20 mM Tris-HCl (pH 7.6). The activity of poly(U)-dependent polyphenylalanine synthesis was followed according to Nierhaus and Dohme [17].

2.7. Modified Scatchard plot

If the binding of Mg^{2+} leading to proton release occurs on homogeneous binding sites obeying the mass action law with the same apparent dissociation constant (K_{app}), then the number (n) of protons released by a jump of the Mg^{2+} concentration from zero to a given concentration $[Mg^{2+}]$ satisfies the Scatchard equation

$$n = n_{max} - K_{app}\frac{n}{[Mg^{2+}]}, \quad (1)$$

where n_{max} is the number of protons released in the limit $[Mg^{2+}] = \infty$. In the case of ribosome, the initial concentration of Mg^{2+} ($[Mg^{2+}]_0$) cannot be made zero because complete elimination of Mg^{2+} leads to denaturation of ribosomes. However, the mass action law yields the following modified Scatchard equation for a jump of the Mg^{2+} concentration from $[Mg^{2+}]_0$ to $[Mg^{2+}]$:

$$n - n_0 = (n_{max} - n_0) - (K_{app} + [Mg^{2+}]_0) \times \frac{n - n_0}{[Mg^{2+}] - [Mg^{2+}]_0}. \quad (2)$$

where n_0 is the number of protons released by the jump of Mg^{2+} concentration from 0 to $[Mg^{2+}]_0$. $n - n_0$ is the observable number of protons released by the jump of Mg^{2+} concentration from $[Mg^{2+}]_0$ to $[Mg^{2+}]$. The plot of $n - n_0$ vs. $(n - n_0)/([Mg^{2+}] - [Mg^{2+}]_0)$ gives a straight line with the ordinate intercept at $n_{max} - n_0$ and a slope of $-(K_{app} + [Mg^{2+}]_0)$. n_{max} can be obtained from the $n_{max} - n_0$ and K_{app} thus determined by using the following equation,

$$n_{max} - n_0 = \frac{K_{app}}{K_{app} + [Mg^{2+}]_0} n_{max}. \quad (3)$$

3. Results and discussion

3.1. Activity of 70 S ribosome

To check the integrity of ribosomes subjected to the unbuffered condition necessary for potentiometric measurement, poly(U)-dependent polyphenylalanine synthesis activity was measured after dialysis at 4°C for 4 h against unbuffered solution with 100 mM KCl and 10 mM $MgCl_2$ at pH $\approx$ 7.6. The unbuffered sample was as active as the control without effect from the unbuffered condition. The activity of 70 S particle formation measured by sucrose gradient centrifugation was about 80 and 65–75%, before and after potentiometric measurement respectively. Thus, our pH titration and proton release data are considered to reflect mainly functionally active ribosome.

3.2. pH titration measurement

The numbers of titrable groups in 70 S ribosome, the rRNA mixture and ribosomal protein mixture were measured by pH titration. The pH titration experiments were carried out in the presence of 100 mM KCl, unless otherwise mentioned.

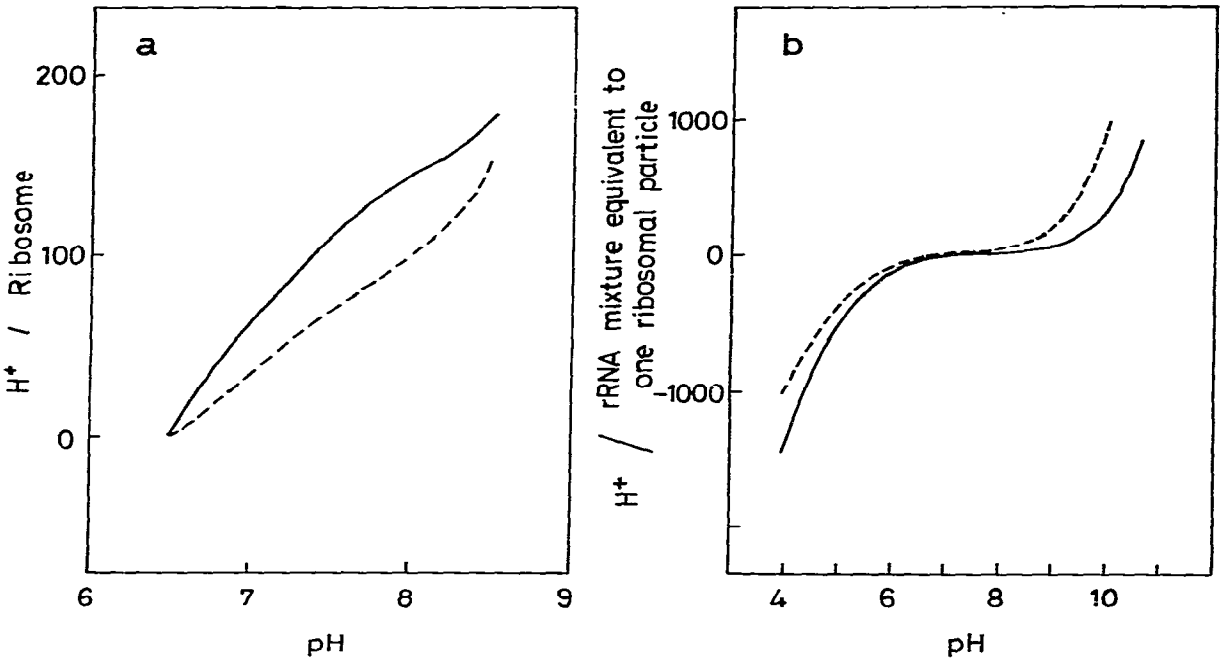

Fig. 1. pH titrations of 70 S ribosome and rRNA mixture in 100 mM KCl at 25°C. (a) Ribosome in 1 mM (———) and 10 mM (- - - - -) $MgCl_2$. The origin of the ordinate was chosen arbitrarily at the initial point of the titrations at pH 6.5. (b) rRNA mixture in 0 mM (———) in 10 mM (- - - - -) $MgCl_2$. The amount of titrated protons was normalized per 70 S ribosome or per 70 S particle equivalent amount of the rRNA mixture.

3.2.1. Ribosome

The pH titration measurements of 70 S ribosome were performed in the pH range between 6.5 and 8.5, where the ribosome is stable, with 1 and 10 mM $MgCl_2$ (fig. 1a). The number of net proton charges titrated in this pH range was about 150 for each curve. The titration curves showed no clear stepwise titrations. Both of the plots at 1 and at 10 mM Mg^{2+} curved upward and downward but this feature was not clear enough to unambiguous determination of titrable groups.

3.2.2. rRNA

Fig. 1b shows the pH titration curves of the rRNA mixture with 0 and 10 mM $MgCl_2$ over the range pH 4- 10. Titration at alkaline pH values was made as quickly as possible to avoid alkali hydrolysis of rRNAs; hydrolysis was less than 10% measured by sucrose gradient centrifugation. The titration curves clearly show the basic and acidic ionizations of nucleotide bases in the acid range pH < 6 and the alkaline range pH > 9, respectively. The pK_a values of bases in the presence of 10 mM Mg^{2+} were shifted toward the low-pH side compared to those in 0 mM Mg^{2+}. The shifts of the pK_a values of bases by Mg^{2+} cannot be ascribed to secondary structure formation by hydrogen bonding. The shift of pK_a by secondary structure formation is toward the acid side for the basic ionization but toward the alkaline side for the acidic ionization as is known for DNA [18], whereas the observed pK_a shifts in rRNA are toward the acid pH side in both the basic and acidic ionizations. As we shall show later, the pK_a shifts can be explained by the decrease of the negative Coulombic field from backbone phos-

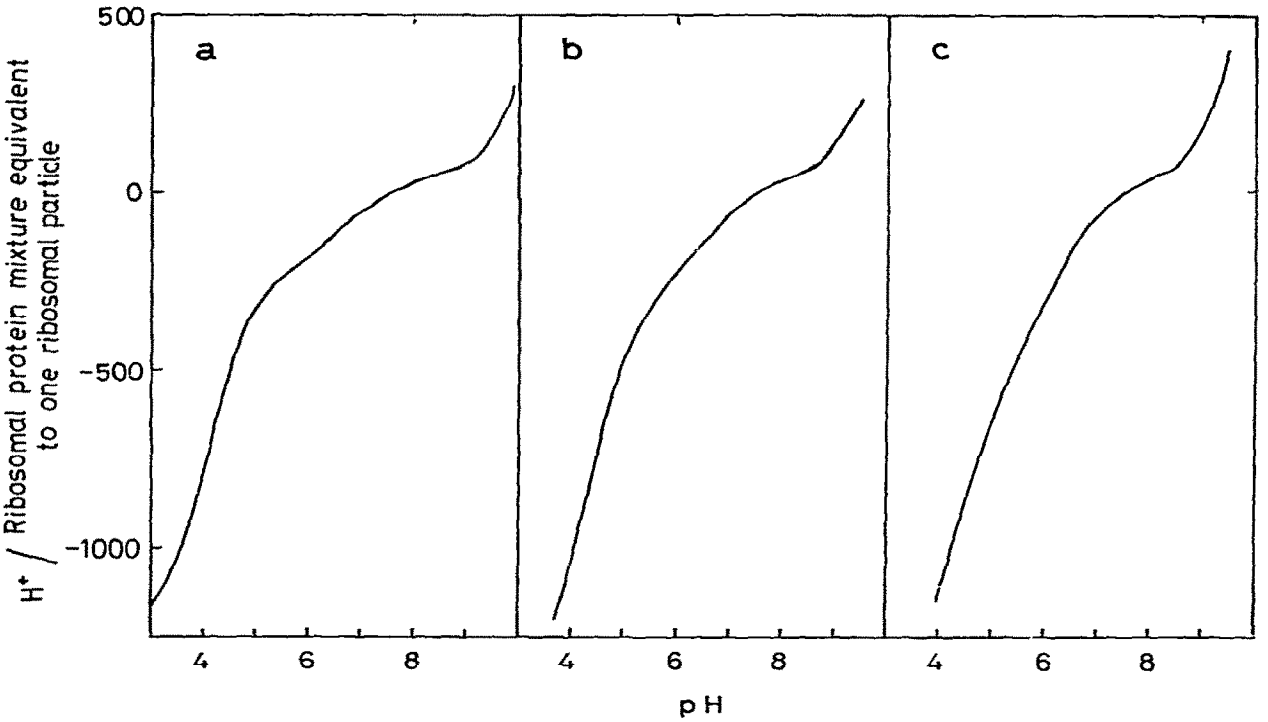

Fig. 2. pH titration of 70 S ribosomal protein mixture dissolved in 6 M (a), 1 M (b) and 0.2 M (c) guanidine hydrochloride at 25°C. The protein solutions of b and c contained 100 mM KCl. The origin of the ordinate was chosen arbitrarily at pH 7.6. The amount of protons was normalized per 70 S particle equivalent amount of proteins.

phates by binding of Mg^{2+} on rRNA.

The net charges in rRNA titrated in the pH region 6.5–8.5 were of the same order (≈ 100) as those in 70 S ribosome (≈ 150), indicating that rRNAs can make a large contribution to the titration of ribosome, in contrast to the suggestion that the titration of ribosome at neutral pH is mainly due to proteins [9].

3.2.3. Ribosomal protein

pH titrations of the ribosomal protein mixture were performed at the three guanidine hydrochloride concentrations of 6, 1 and 0.2 M and with 100 mM KCl except for the case of 6 M guanidine hydrochloride (fig. 2). As the pK_a of guanidine hydrochloride is 13.6 [19], the titrations were made in the pH region below 10.

The number of protons titrated in the region pH 6.5–8.5 was about 200 which was of the same order as that of rRNA. The titration curves of the ribosomal protein mixture showed no change in the presence or absence of Mg^{2+} (data not shown). In the presence of 6 M guanidine hydrochloride where most proteins were denatured, three distinct ionizations at pH ≈ 4, ≈ 6.5 and > 10 were observed. These may correspond to the ionizations of carboxyl groups, imidazole and α-amino groups, and ϵ-amino, phenol and SH groups, respectively. In 1 and 0.2 M guanidine hydrochloride, where ribosomal proteins were renatured to some extent [20], a large fraction of carboxyl groups appeared to have pK_a shifted to the alkaline side (up to pH ≈ 5). Since ribosomal proteins in general have very low solubilities in many buffers and were thus turbid when the concentration of guanidine hydrochloride was lowered to less than about 0.2 M, we

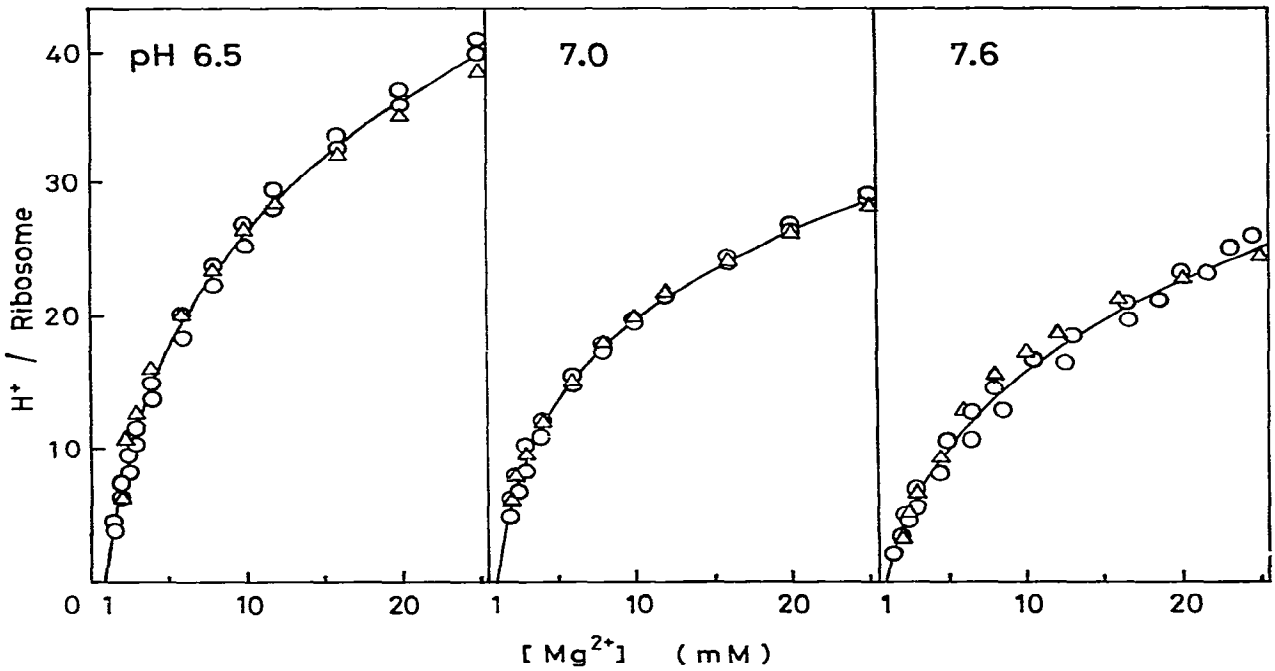

Fig. 3. Mg^{2+} concentration dependence of the proton release from a 70 S ribosome at pH 6.5, 7.0 and 7.6 measured at 25°C. All the ribosome solutions contained 100 mM KCl and initially 1 mM (○) or 2 mM (△) $MgCl_2$. 2 M $MgCl_2$ was added stepwise. The ordinate of △ was shifted so as to bring the initial point of △ on the ○ point at 2 mM Mg^{2+}. The solid curves are traces through the experimental points.

could not make titration measurement of ribosomal proteins in solution completely free from denaturant. However, the data suggest that a large fraction of carboxyl groups have abnormally high pK_a values in the native ribosomal proteins.

3.3. pH-stat measurements of Mg^{2+}-induced proton release

Mg^{2+}-induced proton release was measured by the pH-stat method for 70 S ribosome, the rRNA mixture and the protein mixture in the presence of 100 mM KCl.

3.3.1. Ribosome

Fig. 3 shows how the number of protons released from a 70 S ribosome depends on the Mg^{2+} concentration in a series of Mg^{2+} concentration jumps from the initial Mg^{2+} concentration of 1 or 2 mM. To observe the pH dependence of the proton release, we show in fig. 3 the data measured at three pH values: 6.5, 7.0 and 7.6. We also measured proton release at pH > 8 but the data had a larger error owing to poor stability of the pH of the ribosome solution at alkaline pH, these data are therefore not shown here. Precise measurement of the proton release is usually much more difficult than the pH titration because the number of protons involved in the proton release is much less than that involved in the pH titration.

A 70 S ribosome released about 36 (pH 6.5), 26 (pH 7.0) and 23 (pH 7.6) protons in the Mg^{2+} concentration change from 1 to 20 mM (fig. 3). Thus, 70 S ribosome releases more protons at acid pH than at neutral pH. The proton release curve originating from 2 mM Mg^{2+} overlapped with

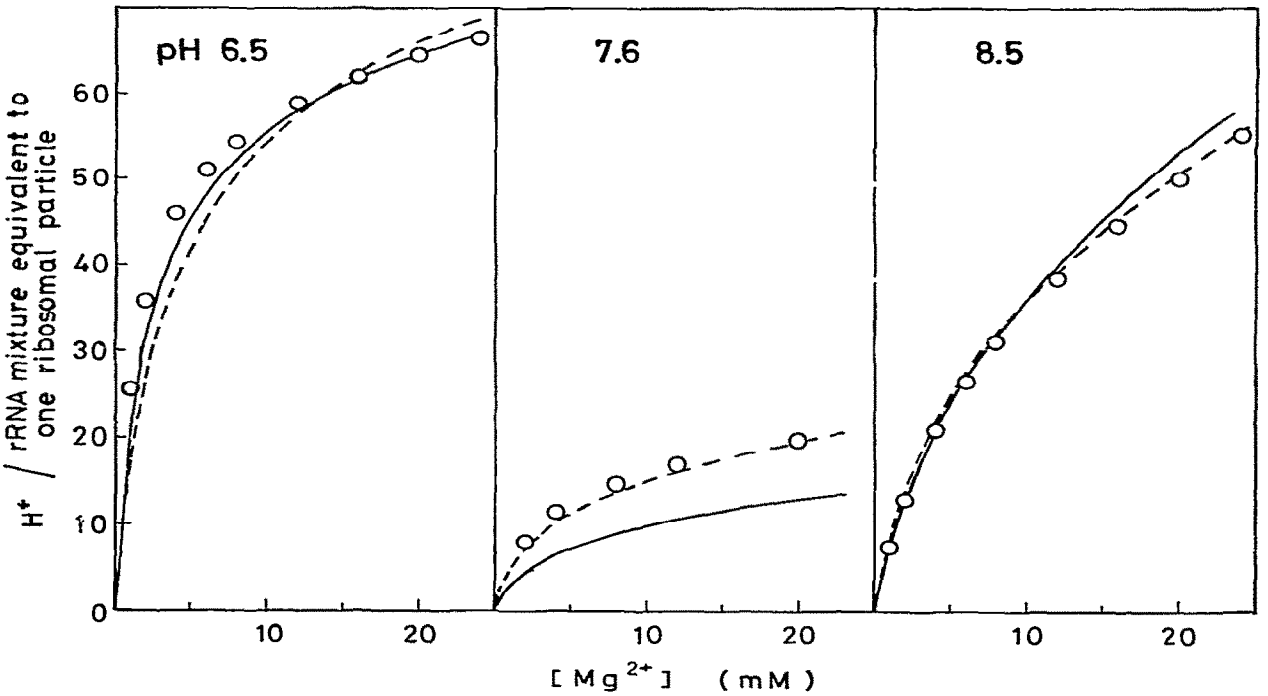

Fig. 4. Mg^{2+} concentration dependence of the proton release from the one 70 S particle equivalent amount of rRNA mixture at pH 6.5, 7.6 and 8.5 measured at 25°C (○). All the rRNA solutions contained 100 mM KCl but initially no Mg^{2+}. 2 M $MgCl_2$ was added stepwise. The solid and dashed lines show the theoretical proton release curves calculated by the two-phase approximation model of electrostatic atmospheric binding of small ions to rRNA with the parameters $pK_0^B = 4.2$, $pK_0^{\wedge} = 8.7$, $\gamma = 0.39$ (———) and $pK_0^B = 5.0$, $pK_0^{\wedge} = 8.05$, $\gamma = 0.115$ (- - - - - -). The parameter a for 16 S rRNA is 70 Å in both curves. Details of the model are described in the text.

that from 1 mM Mg^{2+} within experimental error (fig. 3). The activity of 70 S particle formation is lost on exposure to low Mg^{2+} concentrations and the inactivation is more enhanced at 1 mM Mg^{2+} than at 2 mM Mg^{2+} [16]. Hence, exposure of ribosome to an initial low Mg^{2+} concentration might affect proton release. However, our data show that the initial low Mg^{2+} concentration has little effect on proton release under our experimental conditions.

3.3.2. rRNA

Fig. 4 shows proton release curves of the rRNA mixture for an initial Mg^{2+} concentration of 0 mM measured at pH 6.5, 7.6 and 8.5. Because of the greater stability of the pH in rRNA solution as compared to the ribosome solution, measurement at the alkaline pH 8.5 was also possible. The number of protons released from a unit amount of rRNA mixture with one molecule each of 23 S, 16 S and 5 S components was about 65 (pH 6.5), 20 (pH 7.6) and 50 (pH 8.5), respectively, in the Mg^{2+} concentration change from 0 to 20 mM. The corresponding values for the Mg^{2+} concentration change from 1 to 20 mM were 39 (pH 6.5), 14 (pH 7.6) and 43 (pH 8.5). Thus, the number of protons released from the rRNA mixture and its pH dependence are similar to those of ribosome.

Proton release from rRNA has a rather sharp pH dependence. The number of protons is minimal at the neutral pH 7.6 and increases in both the acid and alkaline pH regions. This marked pH

dependence of proton release cannot be ascribed to a pH-dependent change of the rRNA conformation. The absorbance change at 260 nm of the rRNA mixture in the range pH 6.5–8.5 was observed to be very small ($< 2\%$) in the presence of 100 mM KCl at any constant Mg^{2+} concentration below 20 mM (data not shown).

3.3.3. Ribosomal protein

The ribosomal protein mixture showed no detectable proton release or uptake on addition of Mg^{2+}. This and the pH titration data, which showed no effect of Mg^{2+}, indicate that Mg^{2+} does not bind appreciably to ribosomal proteins and does not have a significant effect on their conformations even in the case of significant binding.

From the above data, we can conclude that the main source of the Mg^{2+}-induced proton release from ribosome is rRNAs and not ribosomal proteins, in contrast to the suggestion of Kliber et al. [9].

3.4. Mechanism of the proton release

Fig. 5a and b shows the modified Scatchard plot and the Scatchard plot of the data in figs. 3 and 4, respectively. All modified Scatchard plots for ribosome and the Scatchard plots for rRNA are not linear but concave upward. This indicates that the Mg^{2+}-binding sites leading to proton release are either heterogeneous or have a negative cooperative interaction [21].

Cation binding to RNA has been most extensively studied for tRNA. The Scatchard plot for divalent cation binding to tRNA was generally found to be concave upward in the presence of monovalent cations [22–26]. This was interpreted as being due to either the existence of at least two classes of cation-binding sites with different binding strengths [27] or a negative cooperative interaction between binding sites that arises from the polyelectrolytic nature of cation binding [28–30]. In the following we shall examine these two possibilities for Mg^{2+}-induced proton release in the simpler case of rRNA.

3.4.1. Hetergeneous Mg^{2+}-binding model

We first examine a model assuming the presence of two classes of Mg^{2+}-binding sites with different binding strengths. A curved (modified) Scatchard plot in fig. 5 can be decomposed into two linear plots as indicated by the dashed lines. The composite (modified) Scatchard curve calculated from the two linear plots [21], show by the solid line in fig. 5, agrees nicely with the observed curve. Therefore, the assumption of two classes of Mg^{2+}-binding sites seem plausible.

Table 1

K_{app} and n_{max} of rRNA estimated by the heterogeneous Mg^{2+}-binding model

pH	Strong binding		Weak binding	
	K_{app} (mM)	n_{max}	K_{app} (mM)	n_{max}
6.5	1.26	53	14.0	25
7.6	0.95	6	7.9	19
8.5	3.13	21	33.0	88

Applying the Scatchard equation (eq. 1) to each dashed linear plot in fig. 5b, we estimated the values of n_{max} and K_{app} for the two classes of Mg^{2+}-binding sites in rRNA. The result is shown in table 1. The table shows the K_{app} and n_{max} have a minimum at neutral pH near 7.6 and increase in both the acid and alkaline pH regions for both the strong and weak binding cases. This pH dependence, however, is difficult to explain by a simple model as we shall see below.

A possible mechanism of proton release is that binding of an Mg^{2+} induces a shift of the pK_a values of nearby ionizable groups B_i ($i = 1, 2, \ldots, n$) via a direct interaction of bound Mg^{2+} or a conformational change as shown in the following scheme:

$$\begin{array}{ccc} HB_iR & + Mg^{2+} \rightleftharpoons & HB_iRMg^{2+} \\ K_i \downarrow & & \downarrow K_i' \\ B_iR & + Mg^{2+} \underset{K_1}{\rightleftharpoons} & B_iRMg^{2+} \end{array} \qquad (I)$$

where R denotes rRNA and K_1 is the intrinsic dissociation constant of Mg^{2+}. K_i and K_i' are the intrinsic proton dissociation constants of an ionizable group B_i before and after binding of Mg^{2+}, respectively. Scheme I is the simplest but most reasonable mechanism of proton release or uptake by ligand binding [31]. The expressions of K_{app}

and n_{max} in scheme I are

$$K_{app} = \left(\prod_i^n \frac{1+[H^+]/K_i}{1+[H^+]/K_i'} \right) K_1 \quad (4)$$

$$n_{max} = \sum_i^n \left(\frac{[H^+]}{K_i+[H^+]} - \frac{[H^+]}{K_i'+[H^+]} \right) = -\frac{d\log K_{app}}{dpH}. \quad (5)$$

Eq. 5 shows that each ionizable group B_i has a bell-shaped contribution to n_{max}. Therefore, the pH dependence of n_{max} as shown in table 1 can be explained by assuming two kinds of ionizable groups, B_1 and B_2, one with proton dissociation constants in the acid pH range, the other in the alkaline pH range. The pH dependence of K_{app}, on the other hand, cannot be explained by scheme I. In the case of proton release, n_{max} is positive. Then, the second expression of eq. 5 shows that K_{app} always decreases with pH. In scheme I, an increase of K_{app} with pH is allowed only in the case of proton uptake. Thus, scheme I contradicts the observed increase of K_{app} at alkaline pH (table 1). Therefore, the model assuming two classes of Mg^{2+}-binding sites and scheme I is unable to explain the proton release from rRNA. It might be possible to construct a consistent model by introducing more than two classes of Mg^{2+}-binding sites including the case of proton uptake or a more complicated scheme. However, such models have little practical value due to too many ambiguities.

3.4.2. Evaluation of the electrostatic potential in rRNA

RNA is a polyelectrolyte with anionic charges on the phosphate backbone. The electrostatic potential produced by the backbone has a decisive influence on the binding of small ions and affects also the ionization of nucleotide bases. Binding of small ions modulates the potential and a change in the potential gives rise to a change in the ionization of bases, thus giving rise to proton release. In the following, we shall consider the electrostatic mechanism of proton release from RNA. Here, we evaluate the potential in rRNA and its effect on the pK_a values of bases.

Theory of the electrostatic field effect in polyelectrolytes has been developed based on the model of atmospheric binding of counterions [28,29]. The atmospheric binding model was applied to the interaction of DNA with small ions [29]. Another model with emphasis on the site binding of counterions was proposed for tRNA [30]. We evaluate the potential for both models.

To calculate the potential in the atmospheric binding model, we use the following two-phase approximation [28]. We assume that an rRNA molecule is coiled into a sphere of radius a and apparent volume $v = 4\pi a^3/3$ and that the electrostatic potential ψ in the sphere is uniform (fig. 6). In dilute solution, the concentration $[M^z]_{in}$ of small ion M^z with charge ze in the free volume inside the sphere is given by

$$[M^z]_{in} = [M^z]_0 \exp[-ze\psi/kT] \quad (6)$$

where $[M^z]_0$ is the free concentration of ion M^z, k Boltzmann's constant and T the absolute temperature. Let us consider the solution with the ions K^+, Mg^{2+} and Cl^-. Then, the total charge N_+e of the small ions contained in the sphere is

$$N_+ = \{[K^+]_0 \exp(-e\psi/kT) + 2[Mg^{2+}]_0 \exp(-2e\psi/kT) - [Cl^-]_0 \exp(e\psi/kT)\}(v - v_0)A_0. \quad (7)$$

where A_0 is Avogadro's number and v_0 the net volume occupied by the rRNA molecule so that $v - v_0$ is the free volume for capture of small ions. The sphere has net charge $-N^*e = -(N - N_+)e$, where N is the number of phosphate groups in the rRNA molecule. The potential ψ is determined so as to be equal to the Debye-Hückel potential at the surface of the sphere

$$\psi = -\frac{N^*e}{4\pi\epsilon_0\epsilon}\left(\frac{1}{a} - \frac{1}{a+\lambda}\right),$$

$$\lambda = (2e^2I/\epsilon_0\epsilon kT)^{-1/2}. \quad (8)$$

where ϵ_0 and ϵ are the dielectric constant of a vacuum and the relative dielectric constant of water, respectively. λ the Debye length and I the ionic strength. From eqs. 7 and 8, ψ is determined as a function of $[K^+]_0$ and $[Mg^{2+}]_0$. In the presence of the potential ψ, the pK_a of an ionizable group in the sphere is shifted by

$$pK_\psi - pK_0 = -e\psi/2.303kT, \quad (9)$$

where pK_0 is the intrinsic pK_a in the absence of

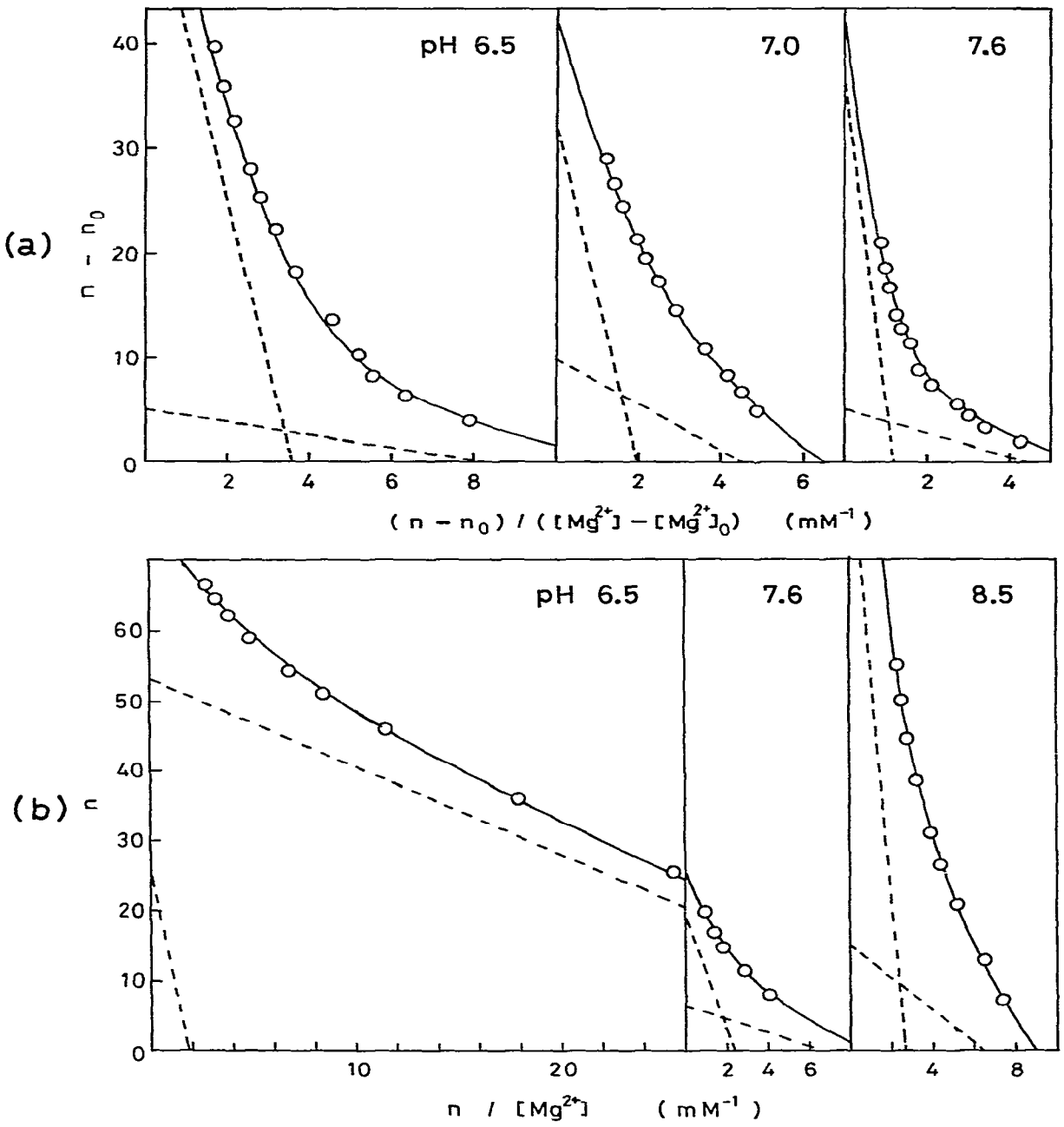

Fig. 5. (Modified) Scatchard plot of the proton releases of 70 S ribosome (a) and the rRNA mixture (b). The proton release data in figs. 3 and 4 are replotted according to eq. 2 (a) and eq. 1 (b), respectively. Only the data in fig. 3 with the initial Mg^{2+} concentration of 1 mM are used in a. The dashed lines show the optimal decomposition of each curved (modified) Scatchard plot into two linear plots. The solid lines show the calculated curves by superposing the two linear plots.

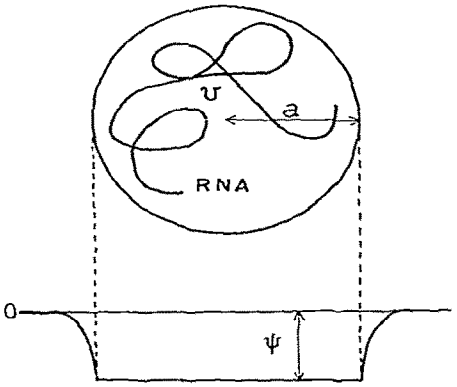

Fig. 6. The two-phase approximation model for the electrostatic atmospheric binding of small ions to rRNA. An rRNA molecule is approximated by a sphere penetrable by small ions and with a uniform inside electrostatic potential.

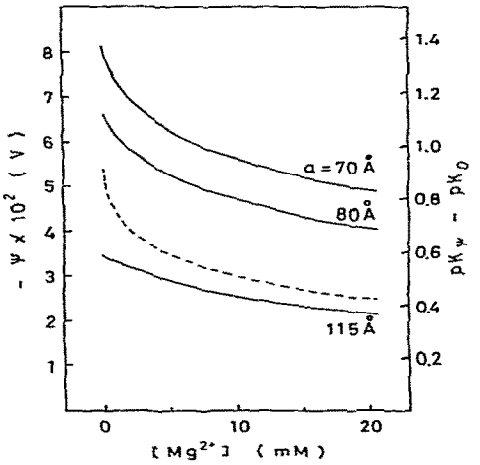

Fig. 7. The electrostatic potential of rRNA calculated by the two-phase approximation model (———) and by the Leroy and Guéron model (- - - - -). The calculations were carried out for the solution with $[KCl]_0 = 0.1$ M and $[MgCl_2]_0$ varying from 0 to 20 mM. In the two-phase approximation model, the potentials for the three cases of 16 S rRNA with radius $a = 70$, 80 and 115 Å are shown. The parameters in the Leroy and Guéron model are given in the appendix.

the potential and pK_ψ the apparent pK_a in the presence of ψ.

We calculated the potential ψ for 16 S and 23 S rRNAs in a solution containing 0.1 M KCl and $MgCl_2$ varying from 0 to 20 mM. We used the phosphate number, $N = 1541$ (16 S) and 2904 (23 S [32], and the net volume $v_0 = 5.2 \times 10^{-22}$ l (16 S) and 1.04×10^{-21} (23 S) calculated from the partial specific volume v_i or rRNA, $v_i = 0.57$ ml/g [33a], and molecular weight 0.55×10^6 (16 S) and 1.1×10^6 (23 S) [33b]. The radius a of the sphere was the only adjustable parameter. If 16 S and 23 S rRNAs have a values such that they give the same charge density in the apparent volume, i.e., N (16 S)/v (16 S) = N (23 S)/v (23 S), then they have almost the same potential. We assume this condition, i.e., a (23 S) = 1.24a (16 S).

Fig. 7 shows the result of the calculation. The radius is represented for 16 S rRNA. The potential is stronger and the change induced by Mg^{2+} is larger for smaller a. The pH titration of rRNA (fig. 1b) shows that pK_a values of bases shift by about 0.3–0.6 upon the Mg^{2+} concentration change from 0 to 10 mM. To explain the observed pK_a shift, a must be 85–60 Å for 16 S rRNA. This value of the radius is smaller than that of 115 Å determined from hydrodynamic measurement under a high-salt condition [34]. This means that the effective volume for the atmospheric binding of small ions is smaller than the hydrodynamic effective volume. The potential in the hydrodynamic effective volume is certainly not uniform because it is much larger than the net volume of rRNA. The bound ions are under the influence of the strong potential near the rRNA chain so that the effective ion binding volume estimated by simple two-phase approximation becomes smaller than the hydrodynamic volume.

In eq. 8 we have used the Debye-Hückel approximation that is questionable for the macroion. However, we note that the potential ψ is rather insensitive to the expression of the right-hand side of eq. 8. For instance, even if we replace the factor $1/a - 1/(a + \lambda)(= (1/10)1/a)$ by $1/a$, ψ changes by only a few percent. This is because the net charge determined by eq. 7 changes rather sensitively according to change of the right-hand side expression of eq. 7 so as to suppress a large change in the value of ψ.

In the above atmospheric binding model, small ions are assumed to be trapped, but mobile within the free volume inside the sphere bounding the coil

of an RNA molecule. Leroy and Guéron [30] proposed a different model for the binding of small ions to tRNA. They represented tRNA as a collection of structural blocks which were approximated by spheres of the same size and assumed to be electrically shielded. Small ions were assumed to experience only the electrostatic field of a sphere and to bind tightly to binding sites on the sphere. This model may be valid for rRNA because rRNA under our solvent condition is not a simple random coil but certainly has many local rigid structures as judged from circular dichroism data [35,36]. Therefore, we also examined the Leroy and Guéron model for rRNA. Details of this model are described in the appendix. We also show in fig. 7 the electrostatic potential on the sphere of a structural block calculated from the Leroy and Guéron model with an appropriate parameter set. We observe that the Mg^{2+} dependence of the potential in the Leroy and Guéron model is similar to that in the atmospheric binding model with $a = 70$ Å which gives a reasonable fit to the proton release data as we shall show in the next section. Therefore, both models are equally able to explain the Mg^{2+}-induced pK_a shift of bases and proton release in rRNA. We cannot decide which is the better model from our experimental data alone.

3.4.3. Proton release by the electrostatic field effect

Let the potentials in the presence and absence of Mg^{2+} be ψ and ψ_0, respectively. Ionizable groups under the influence of the potential make the pK_a shift by

$$pK_\psi - pK_{\psi 0} = -e(\psi - \psi_0)/2.303kT. \quad (10)$$

Since $\psi - \psi_0 > 0$, the pK_a shift is downward. The deprotonated fraction α_ψ of an ionizable group under the potential ψ is

$$\alpha_\psi = 1/\{1 + 10^{(pK_\psi - pH)}\}. \quad (11)$$

Upon change of the potential from ψ_0 to ψ, the ionizable group releases protons to an extent of $\alpha_\psi - \alpha_{\psi 0}$. Therefore, nucleotide bases in RNA can release protons upon change in Mg^{2+} concentration.

The intrinsic pK_a value of the basic ionizations of adenine (A) and cytosine (C) are in the region pH 3.5–5 and those of the acidic ionizations of guanine (G) and uracil (U) in the region pH 9–9.5 [37]. Hence, for simplicity, we assume that A and C have the same intrinsic pK_a, pK_0^B, and that G and U also have the same value, pK_0^A. Since bases forming base-pairs cannot ionize in the region pH 6.5–8.5, we assume that only the fraction γ of bases, in both the A + C and G + U groups, is ionizable. Let the numbers of A + C and G + U in the total rRNA per 70 S particle be N^B and N^A. In rRNA, $N^A/N = 0.48$ and $N^B/N = 0.52$ where $N = N^A + N^B = 4565$ [32]. Hence, we can put $N^A = N^B = N/2$. Then the proton release per total rRNA of a 70 S particle is

$$n = \frac{N\gamma}{2}\left\{\left(\alpha_\psi^A - \alpha_{\psi 0}^A\right) + \left(\alpha_\psi^B - \alpha_{\psi 0}^B\right)\right\}. \quad (12)$$

where α_ψ^A and α_ψ^B are the deprotonated fraction of G + U and the unprotonated fraction of A + C under the potential ψ, respectively.

Since the fraction of charged nucleotide base in the region pH 6.5–8.5 is small compared to phosphate number as seen in fig. 1b, the ionization of bases does not affect the potential significantly. Using the potential in the atmospheric binding model with $a = 70$ Å, we obtain the theoretical proton release curves at pH 6.5 and 8.5 in good agreement with the observed ones (fig. 4). The parameters we used are $pK_0^B = 4.2$, $pK_0^A = 8.7$ and $\gamma = 0.39$. These theoretical pK_a values are near the intrinsic pK_a values of monomer bases and the fraction γ of ionizable bases is near the observed fraction of unpaired bases [35,36]. Therefore, these parameter values are reasonable.

Since the potential in the Leroy and Guéron model is nearly the same as that of the atmospheric binding model with $a = 70$ Å except for the constant difference by about 0.45 in $pK_\psi - pK_0$ units (fig. 7), the Leroy and Guéron model gives almost the same theoretical proton release curves as those shown in fig. 4 if we use the pK_0^A and pK_0^B values shifted by 0.45, i.e., $pK_0^A = 9.15$ and $pK_0^B = 4.65$.

The electrostatic field mechanism can explain the negative cooperativity in proton release. The potential decreases rapidly in a low Mg^{2+} concentration range but only gradually at higher Mg^{2+} concentrations (fig. 7). This is because divalent

cations at low concentrations very effectively bind to a polyanion and effectively screen its charge so that their binding at high concentrations becomes gradual owing to the screening attained at the lower concentrations. This results in the negative cooperativity in Mg^{2+} binding and Mg^{2+}-induced proton release.

The mechanism can also explain the difference in shape of the proton release curves at pH 6.5 and 8.5. The curve at pH 6.5 rises rapidly at low Mg^{2+} concentrations and turns out to saturate at higher Mg^{2+} concentrations, however, the curve at pH 8.5 displays a much slower rise and slower saturation (fig. 4). At pH 6.5, the basic ionizations of A and C mainly contribute to the proton release. The effective pK_a of A and C, pK_ψ^B, is below pH 6.5 and is displayed even further from pH 6.5 by Mg^{2+}, i.e., $pK_\psi^B - 6.5 < pK_{\psi 0}^B - 6.5 < 0$. Hence, the fraction α_ψ^B is more sensitive to change of the potential ψ at low Mg^{2+} concentrations where pK_ψ^B is near pH 6.5 than at high Mg^{2+} concentrations where pK_ψ^B becomes more distant from pH 6.5 (eq. 11). On the other hand, at pH 8.5, the acidic ionizations of G and U mainly contribute to the proton release. The effective pK_a of G and U, pK_ψ^A, is above pH 8.5 and approaches pH 8.5 in the presence of Mg^{2+}, i.e., $0 < pK_\psi^A - 8.5 < pK_{\psi 0}^A - 8.5$. Hence, α_ψ^A, contrast to α_ψ^B, is less sensitive to change of ψ at low Mg^{2+} concentrations than at high Mg^{2+} concentrations. This difference in potential dependence of α_ψ^B at pH 6.5 and α_ψ^A at pH 8.5 result in different shapes of the proton release curves at pH 6.5 and 8.5.

The electrostatic mechanism can also explain the pH dependence of proton release with a minimum at neutral pH (fig. 4). The ionizations of A + C and G + U contribute to the proton release mainly at the acid and alkaline pH regions near pK_0^B and pK_0^A, respectively. The proton release at neutral pH decreases because the pH is far from both pK_0^B and pK_0^A so that the proton release from both groups is small. The proton release at pH 7.6 calculated by the atmospheric binding model with the above-mentioned parameters is also shown in fig. 4. The calculated proton release is less than that observed though its Mg^{2+} dependence is similar. Provided we use pK_0^A and pK_0^B near their monomer values, the proton release at neutral pH is smaller than that observed if we fit the parameters so as to explain the proton releases in acid and alkaline pH regions.

This disagreement can be remedied by considering the following two possibilities. Firstly, the bases mainly contributing to the proton release in rRNA may have abnormal pK_a values. If those bases have intrinsic pK_a values shifted toward neutral pH, then the proton release at neutral pH is increased because the distances $|pK_0^A - pH|$ and $|pK_0^B - pH|$ decrease at neutral pH. The dashed lines in fig. 4 show the theoretical proton release curves calculated with the parameters $a = 70$ Å, $pK_0^B = 5.0$, $pK_0^A = 8.05$ and $\gamma = 0.115$. Thus, with the pK_a values shifted by about 1 unit toward the neutral pH side from the normal monomer values, we can explain the observed pH dependence of the proton release. Note also that a small value (0.115) for the fraction γ of ionizable bases is enough to explain the proton release if such abnormal bases are really contributing. The above-described abnormal pK_a values estimated by the simple two-phase approximation are not reliable. It is likely that the pK_a values of bases in rRNA are not uniform and some bases have abnormal pK_a values because rRNA is considered to have many local rigid tertiary structures. Secondly, the potential in rRNA is not uniform. If some parts in rRNA have a stronger potential than average, then the $pK_{\psi 0}^B$ in those parts shifts more upward, resulting in more proton release at neutral pH. Both possibilities of inhomogeneous pK_a values and inhomogeneous potentials seem to be equally likely, however, we cannot yet comment on the quantitative aspects except that the inhomogeneity in rRNA appears to have a substantial effect on proton release.

We finally note that in the atmospheric binding model there may be the possibility of the release of protons atmospherically trapped in the effective volume of rRNA. However, because of the very small concentration of H^+ in the region pH 6.5–8.5, the number of H^+ atmospherically trapped in an rRNA molecule is estimated to be smaller than 0.1 and the effect of such protons is negligible.

From the above analyses we can conclude that the main mechanism of the Mg^{2+}-induced proton release from rRNA is not a specific effect of bound Mg^{2+} on ionizable groups but a nonspecific

effect of the electrostatic field of the phosphate groups on ionizations of bases. This phenomenon reflects well the characteristics of rRNA as a polyelectrolyte in having a strong electrostatic field produced by the phosphates in the backbone, which is modulated by the binding of counterions, and in possessing nucleotide bases ionizable in acid (pH 5) and alkaline (pH 9) pH regions.

The main mechanism of proton release from ribosome also is considered to be the electrostatic field effect and the major source of protons appears to be rRNA owing to the marked similarity to the proton release from rRNA. However, its modeling is much more ambiguous than that of rRNA. For instance, a fraction of ionizable amino acids in ribosomal proteins may contribute to proton release, yet another may form salt bridges with phosphates of rRNA and not contribute to it. Because of many such unknown factors, unambiguous modeling of the proton release from ribosome is practically impossible. However, it is certain that ribosomal proteins affect the proton release as seen from the obvious difference in the quantitative aspect of the proton release between ribosome and rRNA.

3.5. Defect of the pH-stat method

The pH-stat method is an established technique for the quantitative detection of proton release and uptake [38,39]. However, a large amount of sample is necessary to obtain a satisfactory quantitative precision. We could not measure separately the proton releases from 30 S and 50 S subunits and 16 S and 23 S rRNAs because of the difficulty in preparing them in sufficient amounts for the pH-stat measurement. To overcome this difficulty, we have developed a new quantitative technique to detect protons with much better sensitivity than the pH-stat method which will be described in a separate paper.

Appendix

We describe here the model of rRNA according to Leroy and Guéron [30]. rRNA is approximated by a collection of impenetrable spheres of the same radius R and mutually screened by counterions. The sphere is considered to be of size similar to that of a structural block in tRNA and is assumed to have 12 phosphates uniformly distributed on the surface. Ionizable bases are also assumed to be distributed uniformly on the surfaces of the spheres.

We consider a solution containing the monovalent cation M_1 ($= K^+$) and the divalent cation M_2 ($= Mg^{2+}$). Let ν_i ($i = 1, 2$) be the numbers of the cations M_i bound to a sphere. The charge of the sphere is

$$\rho(\nu_1, \nu_2) = \sum_{i=1}^{2} z_i \nu_i - 12. \tag{A1}$$

where $z_1 = 1$ and $z_2 = 2$. By assuming uniform distribution of charge on the sphere, the potential on the surface of the sphere is given in the Debye-Hückel approximation as

$$\psi(\nu_1, \nu_2) = \frac{e}{4\pi\epsilon_0\epsilon}\rho(\nu_1, \nu_2)\left(\frac{1}{R} - \frac{1}{R+\lambda}\right). \tag{A2}$$

The probability $P(\nu_1, \nu_2)$ for the sphere to bind ν_i of the cations M_i is

$$P(\nu_1, \nu_2) = m(\nu_1, \nu_2)\prod_{i=1}^{2}([M_i]_0/K_i)^{\nu_i} \times \exp[-W(\nu_1, \nu_2)/kT], \tag{A3}$$

where K_i is the intrinsic dissociation constant of the cation M_i in the binding to phosphate groups, $W(\nu_1, \nu_2)$ is the electrostatic energy of the sphere

$$W(\nu_1, \nu_2) = \frac{e^2}{8\pi\epsilon_0\epsilon}\rho^2(\nu_1, \nu_2)\left(\frac{1}{R} - \frac{1}{R+\lambda}\right), \tag{A4}$$

and $m(\nu_1, \nu_2)$ is the combinatorial number of the binding of the cations M_1 and M_2 to a sphere

$$m(\nu_1, \nu_2) = \binom{12}{\nu_1}\binom{12-\nu_1-\nu_2+1}{\nu_2} \tag{A5}$$

The expression of $m(\nu_1, \nu_2)$ is obtained on the assumption that the monovalent cations are distributed freely on the binding sites but that the divalent cations bind to vacant binding sites with the constraint that any pair of them do not occupy nearest-neighbor sites. The effective potential on the sphere is the statistical average

$$\psi = \sum_{\nu_1,\nu_2}\psi(\nu_1, \nu_2)P(\nu_1, \nu_2)/\sum_{\nu_1,\nu_2}P(\nu_1, \nu_2). \tag{A6}$$

Ionizable bases are assumed to experience this potential.

The potential ψ shown in fig. 7 was calculated from eq. A6 using the dissociation constants K_1 for K^+ and K_2 for Mg^{2+} with the values $K_1 = 1/0.65$ M and $K_2 = 1/8$ M as utilized by Leroy and Guéron [30] and $R = 12$ Å. The value of R is larger than the value 7.8 Å which they used for tRNA but is still reasonable as the size of the structural block with 12 phosphates.

References

1 P. Spitnik-Elson and D. Elson, Progr. Nucleic Acid Res. Mol. Biol. 17 (1976) 77.
2 C. Stahli and H. Noll, Mol. Gen. Genet. 153 (1977) 159.
3 J.A.L.I. Walters and G.A.J. van Os, Biochim. Biophys. Acta 199 (1970) 453.
4 B.E.H. Maden and R.E. Monro, Eur. J. Biochem. 6 (1968) 309.
5 Y.S. Choi and C.W. Carr, J. Mol. Biol. 25 (1967) 331.
6 J.A.L.I. Walters and G.A.J. van Os, Biopolymers 10 (1971) 11.
7 D. Elson, P. Spitnik-Elson, S. Avital and R. Abramowitz, Nucleic Acids Res. 7 (1979) 465.
8 A. Revzin, F. Neumann and A. Katchalsky, J. Mol. Biol. 79 (1973) 95.
9 J.S. Kliber, G. Hui Bon Hoa, P. Douzou, M. Graffe and M. Grunberg-Manago, Nucleic Acids Res. 3 (1976) 3423.
10 K. Horie, A. Wada and H. Fukutome, J. Biochem. 90 (1981) 449.
11 P. Traub, S. Mizushima, C.V. Lowry and M. Nomura, Methods Enzymol. 20 (1971) 391.
12 S.J.S. Hardy, C.G. Kurland, P. Voynow and G. Mora, Biochemistry 8 (1969) 2897.
13 W.E. Hill, G.P. Rossetti and K.E. van Holde, J. Mol. Biol. 44 (1969) 263.
14 R.F. Itzaki and D.M. Gill, Anal. Biochem. 9 (1956) 401.
15 A.E. Martel and M. Calvin, Chemistry of the metal chelate compounds (Prentice-Hall, Englewood Cliffs, NJ, 1956) p. 389.
16 A. Zamir, R. Miskin, Z. Vogel and D. Elson, Methods Enzymol. 30 (1974) 406.
17 K.H. Nierhaus and F. Dohme, Methods Enzymol. 59 (1979) 443.
18 D.O. Jordan, in: The nucleic acids, vol. 1, eds. E. Chargaff and J.N. Davidson (Academic Press, New York, 1955) p. 447.
19 D.O. Gray and P.D.J. Weitzmann, in: Data for biochemical reserach, eds. R.M.C. Dawson, D.C. Elliott, W.H. Elliott and K.M. Jones (Oxford University Press, London, 1969) p. 1.
20 S.H. Allen and K.-P. Wong, Biochemistry 17 (1978) 3971.
21 C.R. Cantor and P.R. Schimmel, Biophysical chemistry part III: The behavior of biological macromolecules (W.F. Freeman, San Francisco, 1980) p. 856.
22 M. Bina-Stein and A. Stein, Biochemistry 15 (1976) 3912.
23 M. Cohn, A. Danchin and M. Grunberg-Manago, J. Mol. Biol. 39 (1969) 199.
24 A. Danchin, Biopolymers 11 (1972) 1317.
25 R. Römer and R. Hach, Eur. J. Biochem. 55 (1975) 271.
26 A.A. Schreier and P.R. Schimmel, J. Mol. Biol. 86 (1974) 601.
27 P.R. Schimmel and A.G. Redfield, Annu. Rev. Biophys. Bioeng. 9 (1980) 181.
28 F. Oosawa, Polyelectrolytes (Marcel Dekker, New York, 1971) and references therein.
29 G.S. Manning, Q. Rev. Biophys. 11 (1978) 103.
30 J.L. Leroy and M. Guéron, Biopolymers 16 (1977) 2429.
31 M. Laskowski, Jr and W.R. Finkenstadt, Methods Enzymol. 26 (1972) 193.
32 F.H. Noller, in: Ribosome: Structure, function, and genetics, eds. G. Chambliss, G.R. Craven, J. Davies, K. Davis, L. Kahan and M. Nomura (University Park Press, Baltimore, 1980) p. 3.
33 a. H. Boedtker, in: Handbook of biochemistry and molecular biology: Nucleic acids vol. II, ed. G.D. Fasman (CRC Press, OH, 1976) p. 405; b. D. Donner, in: Handbook of biochemistry and molecular biology: Nucleic acids vol. II, ed. G.D. Fasman (CRC Press, OH, 1976) p. 471.
34 S.H. Allen and K.-P. Wong, J. Biol. Chem. 253 (1978) 8759.
35 W.B. Gratzer and E.G. Richard, Biopolymers 10 (1971) 2607.
36 R.A. Cox, W. Hirst, E. Godwin and I. Kaiser, Biochem. J. 155 (1976) 279.
37 K. Burton, in: Data for biochemical research, eds. R.M.C. Dawson, D.C. Elliott, W.H. Elliott and K.M. Jones (Oxford University Press, London, 1969) p. 169.
38 J.-R. Garel and B. Labouesse, J. Mol. Biol. 47 (1970) 41.
39 D.M. Glick, Biochemistry 7 (1968) 3391.